

Hand grip force estimation via EMG imaging

Betzalel Fialkoff^a, Harel Hadad^a, Darío Santos^b, Franco Simini^b, Marcelo David^{a,*}

^a Jerusalem College of Technology, Jerusalem, Israel

^b Núcleo de Ingeniería Biomédica, Universidad de la República, Montevideo, Uruguay

ARTICLE INFO

Keywords:

Electromyography
Hand grip force
Functional Imaging

ABSTRACT

Physiological muscle disorders resulting from various diseases, such as sarcopenia or strokes, affect millions of people each year according to the American Heart Association. Medical examinations for assessing muscle health are difficult to administer and lack standardization. Surface electromyography (sEMG) signals have found a wide variety of applications; in this work, we present a simple reliable framework for hand grip force estimation using them. We hope that this work will lay the groundwork for applying hand grip force estimation as a method for standardized and reliable muscle health assessment. Seven healthy male subjects were voluntarily recruited and sEMG signals were collected from eight electrodes uniformly distributed around the forearm. A logarithmic function can describe the EMG–force relationship. We propose a novel method for generating functional potential-based inverse EMG images of the forearm. The hand grip force can be estimated from the reconstructed images. Using a simple lightweight system and simple algorithmic techniques we can attain a mean correlation coefficient of 0.95 ± 0.01 and mean RMSE of $0.18 \pm 0.08N$. The results are presented for subject-dependent tests, the generalizability of the method is still to be researched over a larger cohort of subjects, including rehabilitation patients.

1. Introduction

Degradation or loss of muscle function affects millions of people worldwide. Loss of hand-grasp abilities is one of the effects of neurological accidents (such as strokes). According to the World Health Organization (WHO), post-stroke hemiplegia affects about 15 million people annually around the world [1]. About 30% of stroke victims are unable to regain full control of their extremities to the extent they had before the stroke [1]. Even more, severely conservative estimates show that sarcopenia, a condition characterized by loss of skeletal muscle mass and function, affects more than fifty million people today and will affect more than two hundred million in the next forty years according to the American Health Association [2]. In the US alone the cost of these conditions is estimated to be approximately seventy billion dollars per year [2,3].

Muscle force estimation could have significant implication for muscle health assessment [4,5]. Improved evaluation of muscle force may be used to diagnose muscular disorders, to decide if a patient qualifies for a particular treatment, or to track the effectiveness of a treatment [6,7,4]. Manual muscle testing (MMT) is one of the predominant methods for assessing muscle health [8]. There is a strong need to reach consensus on

definitions for standardized tests of muscle health and methods to easily and rapidly assess muscle health with minimal patient burden are needed [9]. There is increasing demand for objectivity regarding muscle testing and the addition of a simple quantitative measurement protocol as a complement to MMT could be highly advantageous [8].

Electromyography (EMG) is an electrodiagnostic measurement technique for measuring the electrical activity produced by skeletal muscles [10]. An EMG signal is the direct reflection of the action potentials generated in a neuro-muscle junction. For this reason, it is widely accepted that EMG signals can be used as a predictor of muscle force [11,12]. One area that has not been deeply explored is the possibility of using the signal to assess muscle health and in particular, recovery stages in patients following neurological accidents involving functionality of the extremities. The EMG may be measured non-invasively by placing electrodes at the skin's surface which is usually desirable. However, sEMG signals acquire noise while traveling along the muscle through tissues and electrodes may collect signals from different motor units simultaneously. We believe that these factors have inhibited the development of robust systems that can be used in real-world settings.

Potential-Based Inverse Imaging refers to a variety of methods of

* Corresponding author at: Jerusalem College of Technology, Havaad Haleumi 21 St., Jerusalem 9372115, Israel.

E-mail address: marcelod@jct.ac.il (M. David).

<https://doi.org/10.1016/j.bspc.2022.103550>

Received 17 October 2021; Received in revised form 25 January 2022; Accepted 2 February 2022

Available online 8 February 2022

1746-8094/© 2022 Elsevier Ltd. All rights reserved.

tissue imaging using non-invasive measurements of bio-electric potentials [13]. Potential-Based Inverse Imaging has been applied in a variety of research settings such as electromyometrial imaging (EMMI) [14], for predicting preterm birth using EMG signals [13], for EMG source localization [15], for pulmonary vein isolation imaging and [16], for the characterization of myocardial infarction using ECG signals [17].

The most common and widely used form of Potential-Based Inverse Imaging is Electrical Impedance Tomography (EIT) [18]. EIT has been used for monitoring ventilation distribution, assessment of lung over-distension and collapse, and pneumothorax detection [19]. Time difference EIT (td-EIT) refers to EIT measurements between two or more physiological states, e.g. between inspiration and expiration. One benefit of td-EIT is that inaccuracies resulting from inter-individual anatomies, such as insufficient skin contact of surface electrodes, can be ignored because most artifacts will eliminate themselves due to simple image subtraction. As of today, the greatest progress of EIT research has been achieved with td-EIT [20,21,19].

A typical EIT procedure is performed by placing N electrodes encircling the tissue of interest. Current is passed between each pair of electrodes while measuring the voltages induced on the other electrodes. From these measurements, an inverse calculation is performed to determine changes in conductivity across the tissue of interest. These differences in conductivity can be displayed as shades of gray in an image [22].

Mathematically, the problem of recovering conductivity from surface measurements of current and potential is a non-linear inverse problem and is severely ill-posed. The mathematical formulation of the problem is due to Alberto Calderón [23], and is called "Calderón's inverse problem" or the "Calderón problem". EIT is of particular interest to us in this research due to the physical similarities between the EIT measurement protocol and the eight-channel measurement setup used in this research.

One of the force-estimation approaches that have gained some popularity utilizes high-density electrode arrays. Staudenmann et al. (2006) [24] showed that force estimation based on EMG signals collected from high-density electrode arrays offers significant error reduction relative to force estimation from signals collected from individual electrodes. Based on this research Huang et al. (2017) [25] demonstrated a novel algorithm, based on non-negative matrix factorization, for isometric force estimation. The EMG envelope matrix was factorized into a matrix of basis vectors with each column representing an activation pattern and a matrix of time-varying coefficients. Although high-density arrays have been shown to lead to improved force estimation, they are not ideal [26]. They lead to redundancy since many of the electrodes capture similar information, they lead to increased complexity in signal processing, and they increase the cost of the system.

The goal of this research is to use a low-cost eight-channel EMG measurement system to provide a simple algorithmic approach for accurate force estimation which can lead to clinical methods that could complement MMT in determining muscle health.

2. Materials and methods

2.1. The measurement system

The EMG measurement system is an affordable lightweight multi-channel EMG and hand grip-force measurement system developed at our laboratory. The EMG signals are measured using eight Myoware EMG SEN-13723 sensors placed around the forearm with respect to a common reference electrode, placed distal to the other electrodes on the forearm. The EMG DC offset is $+\frac{V}{2}$. Each sensor is connected to a Power supply of +5V and a ground voltage of 0V. The associated hand-grip force is measured using a force-sensing resistor (FSR) which is placed on a DIGI-FLEX such that the FSR is compressed in tandem with the hand exerciser. The system collects nine analog signals which are converted to

digital signals using a 10-bit analog-to-digital converter connected to a Raspberry Pi. The signals are sampled at 1980Hz, amplified, and saved, up to the point of maximal voluntary contraction, for off-line analysis and signal processing. All of the routines, processes, and analyses were performed using python programs written in our lab.

2.2. Informed consent

Seven healthy male subjects were voluntarily recruited in this study. Each subject signed the written informed consent documents before participating in the experiments. All the subjects were healthy and none of them reported any neurological disorders or musculoskeletal problems. The subjects were aged between 22 and 42 years old. The subject's forearms ranged from 27 to 30 cm in length and 22 to 30 cm in circumference. The average participant age is 29 years old. Ethical approval was obtained from the Research Ethics Committee of the *Universidad de la República Hospital (Hospital de Clínicas)*, Montevideo, Uruguay, number 032018.

2.3. Measurement protocol

The primary muscles under observation in this study are the brachioradialis, flexor carpi radialis, flexor carpi ulnaris. Eight MyoWare Muscle Sensors placed radially around the forearm collect EMG signals from the primary muscles, as well as several additional secondary muscles, palmaris longus, flexor digitorum superficialis, extensor carpi ulnaris, extensor digiti minimi, extensor digitorum. Table 1 enumerates the electrodes and the muscles they roughly correspond to. It is noted that, as is always the case when measuring EMG signals, there may be significant crosstalk between the muscles and each electrode doesn't strictly correspond only to the muscle listed. The hand-grip force is measured on a force-sensing resistor (FSR) which is coupled to a Digi-Flex hand exerciser. The FSR is placed so that its active surface is compressed in tandem with the hand exerciser. The subject's hand is held in a relaxed position throughout the compression, which takes approximately 3-7 s. The electrode configuration was done following the procedure described by Baranski and Kozupa (2014) [27]. Figs. 1a and 1b shows the experimental setup and electrode placement used in this study. Subjects were instructed to sit comfortably with their handheld in a relaxed position while performing a compression monotonically increasing force. Subjects performed twenty trials with rest periods to offset muscle fatigue.

2.4. Regression procedure

The subject that participated in this study were instructed to increase the strength of their grip throughout the compression. An analysis of the force profiles revealed that force signals appeared logarithmic and consequently a logarithmic relationship is assumed between features of the eight-channel EMG signal and the measured force. Under this assumption, the force estimation problem can be formulated as a regression problem the measured force is estimated using the eight-element vector of features extracted from each channel of the measured EMG signal.

Table 1
The subject muscles and their corresponding electrodes.

Electrode Number	Muscle Name	Color
1	Palmaris Longus	Blue
2	Flexor Digitorum Superficialis	Green
3	Extensor Carpi Ulnaris	Purple
4	Extensor Digiti Minimi	Orange
5	Extensor Digitorum	Red
6	Brachioradialis	Brown
7	Flexor Carpi Radialis	Black
8	Flexor Carpi Ulnaris	Grey

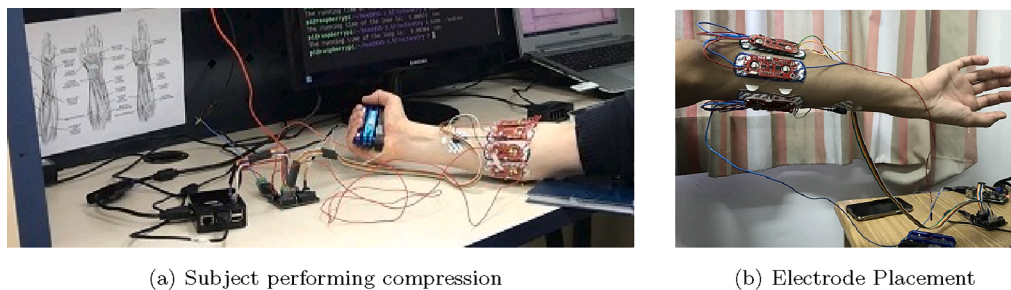


Fig. 1. Experimental setup and electrode placement used in this study.

The accepted method of feature extraction for EMG signals is to segment the signal into overlapping windows and extract a single global feature from each window. When determining the window size, a trade-off must be made between accuracy and temporal resolution. Using windows smaller than 0.2 s generally requires a postprocessing mechanism to make accurate classifications. Larger window sizes are known to increase classification accuracy [26]. To ensure that our windows contain sufficient information for accurate estimation, we chose a window size of 0.25 s with an overlap of 0.125 s. The mean-absolute voltage (MAV) Eq. 1 was chosen as a global window feature as it leads to high EMG-based classification accuracy at a low computational cost [28]. 4th order Butterworth filter with a passband of 20 – 150Hz is applied to each of the eight channels. A brute force search determined that this was the optimal passband, which is in agreement with De Luca et al. (2002) [29] who stated that dominant EMG activity is known to occur in this range. The force signal is filtered by a moving average filter with a kernel length of 500 samples (0.25 s). Samples recorded after the point of maximum voluntary contraction (MVC) were not included in the analysis.

$$MAV = \frac{1}{N} \sum_{i=1}^N |x_i| \quad (1)$$

The features are normalized following standard practice. We chose min–max normalization Eq. 2 to normalize the MAV voltage. Remembering that the logarithm of the normalized MAV will be calculated, we add 1 so that the predicted force is never negative. The signals are windowed and the normalized MAV is calculated in each window for each of the eight channels. The EMG feature vector \vec{V} is fit to a logarithmic function Eq. 4. Eq. 3 shows the final feature vector that is calculated in each window for each of the eight channels. The weight vector \vec{W} are the parameters of the model which transform the feature vector into the estimated force. \vec{W} is computed using an ordinary least squares regression.

$$\bar{X} = \frac{X - X_{min}}{X_{max} - X_{min}} \quad (2)$$

$$\vec{V} = \log(\overline{MAV} + \vec{1}) = \left[\log(\overline{MAV}_1 + 1), \dots, \log(\overline{MAV}_8 + 1) \right] \quad (3)$$

$$\begin{aligned} F &= \vec{W} \cdot \vec{V}^T \\ \vec{W} &= [w_1, w_2, \dots, w_8] \end{aligned} \quad (4)$$

2.5. Image reconstruction

EIT uses the voltage difference between an electrode and all other electrodes to generate the image. Inspired by this, we similarly calculate, at each time step, the voltage difference between a given electrode and the other electrodes; this is repeated around all eight electrodes. This process yields an 8×8 matrix V which is shown by Eq. 5. The matrix V is then flattened into a 64×1 array of voltage differences for each segment of the EMG signals. We refer to this as the pairwise voltage difference

vector. We used the open-source EIT framework EIDORS [30] to solve the inverse conductivity problem. In EIT the surface voltage measurements would be used to solve the inverse EIT problem [23]. We used the pairwise voltage vectors in place of these. This procedure generates an image that might represent functional imaging showing the activation of the subject muscles. This method utilizes the EIT reconstruction algorithm as the basis for a form of PIE imaging.

$$v_{ij} = V_i - V_j \quad i, j \in [1, 8] \quad (5)$$

2.6. Vision transformers

Transformers are a deep learning model that adopts the mechanism of attention, differentially weighing the significance of each part of the input data. Transformers are designed for sequence-to-sequence tasks such as translation and text summarization. They are used primarily in the field of natural language processing (NLP) and have recently been adapted and implemented for Computer Vision problems [31–33].

In computer vision tasks an image is tokenized into small grids of pixels typically 8×8 or 16×16 . The patches' positions are encoded, to retain information regarding the proximity of one patch to another, and then passed into the transformer network. In this research, we used a Vision Transformer (ViT) network implemented in the PyTorch framework [34]. An image is split into fixed-size patches. Each patch is linearly and positionally embedded. The resultant sequence of vectors is fed to a standard Transformer encoder [35]. To use this model for regression instead of classification we use the standard approach of removing the classification layer. An overview of the model is depicted in Fig. 2 reproduced from [36] (Apache-2.0 License). In the original work, a patch size of 16×16 pixels was used. Our images are 64×64 pixels which are significantly smaller. Therefore we used a patch size of 4×4 pixels. All the signals were randomly split between a training and validation set. The split was performed such that each of the twenty signals collected from each subject was split 70%-30% so that in each subject had fourteen signals used for training and six signals used for validation.

3. Results

3.1. Logarithmic model

The EMG signals from each subject were independently fitted to the logarithmic model given in Eq. 4, mean correlation coefficients and root-mean-square errors (RMSE) are calculated yielding a mean correlation coefficient of 0.95 ± 0.04 and mean RMSE of $0.18 \pm 0.12N$. Table 2 shows the mean correlation coefficients and root-mean-square errors for each subject. Fig. 3 shows an example of the logarithmic model applied to a compression.

3.2. Potential based inverse electromyography imaging

3.2.1. Image reconstruction

The raw EMG signals were segmented into 0.25-s segments and the MAV was extracted. The pairwise voltage difference is calculated

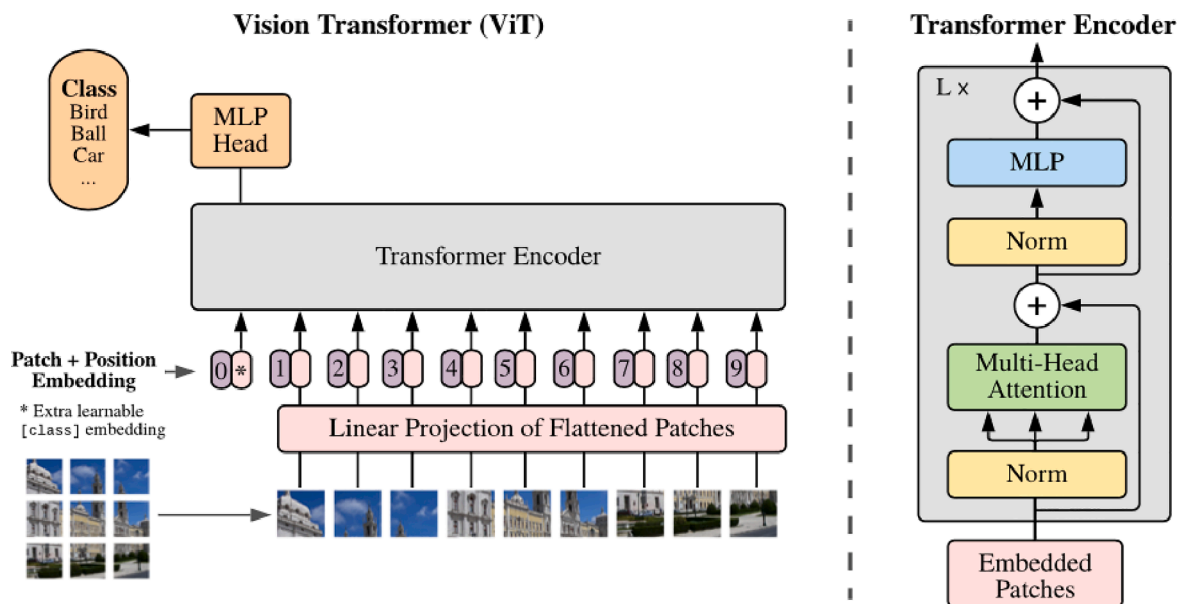


Fig. 2. Overview of the ViT model. Reproduced from [36] under the Apache 2.0 license.

Table 2
Mean correlation coefficients and RMSE for each subject, logarithmic model.

Subject	Logarithmic Model	
	Mean R^2	Mean RMSE
1	0.97	0.21
2	0.96	0.14
3	0.94	0.24
4	0.96	0.08
5	0.94	0.15
6	0.95	0.13
7	0.97	0.31
All	0.95	0.18

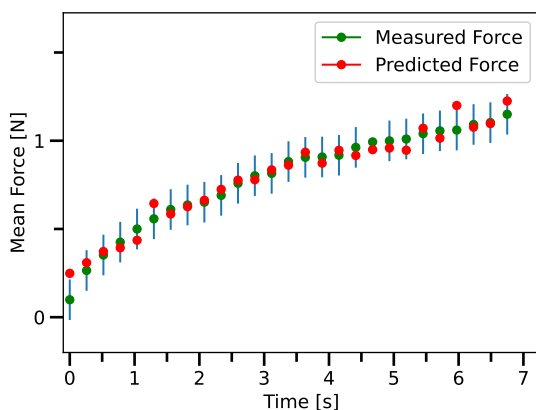


Fig. 3. An example of the force estimated over the course of a single compression using the logarithmic model Subject 4.

according to the procedure described in Section 2.5. The compression is now represented by a series of tomographic images. The first image in the series is subtracted from subsequent frames so that the images reflect evolution over time. Fig. 4 shows the reconstructed functional EMG images.

3.2.2. Image analysis

The value of the brightest pixel on the reconstructed image (before

color-mapping) is extracted and fitted to the logarithmic model given in Eq. 4. Mean correlation coefficients and root-mean-square errors (RMSE) are calculated yielding a mean correlation coefficient of 0.91 ± 0.06 and mean RMSE of $0.23 \pm 0.12N$. Table 3 compares the mean correlation coefficients and root-mean-square errors obtained for each subject. Fig. 5 shows an example of the logarithmic model applied to the features extracted to the images generated from a compression.

3.3. Vision transformers

Table 4 shows the mean correlation coefficients and root-mean-square error (RMSE) for each of the subject. Mean correlation coefficients and root-mean-square errors (RMSE) are calculated yielding a mean correlation coefficient of 0.95 ± 0.03 and mean RMSE of $0.27 \pm 0.07N$. Figs. 6 shows an example of the ViT model applied to a compression.

4. Discussion

Muscle force is often used as a proxy for muscle health and is highly correlated to it. We suggest that EMG-based analyses may have many positive implications for muscle health assessment and may provide a framework for standardized, quantitative muscle health assessments. In this research, we explore the feasibility of using EMG-based analyses to complement MMT procedures by attempting to model the muscle force using the EMG signal and attempting to estimate the muscle force using information extracted from the EMG signal.

We present two distinct methods for modeling the relationship between the muscle force and the associated eight-channel EMG signal. In the first method, we showed that the logarithm of the MAV feature vector of a windowed EMG signal is highly correlated to the mean force. Using this method we obtained a mean correlation coefficient of 0.95 ± 0.04 and mean RMSE of $0.18 \pm 0.12N$.

The second method is based on the similarity between our experimental setup and the EIT procedure. Noting this similarity we demonstrated a novel method of EMG-based image reconstruction using the EIT reconstruction algorithm, i.e Calder's Problem. We showed that the logarithm of certain images features are also highly correlated to the mean force. Using this method we obtained a mean correlation coefficient of 0.91 ± 0.06 and mean RMSE of $0.23 \pm 0.12N$. We believe that this indicates that the image represents the degree of muscle activation

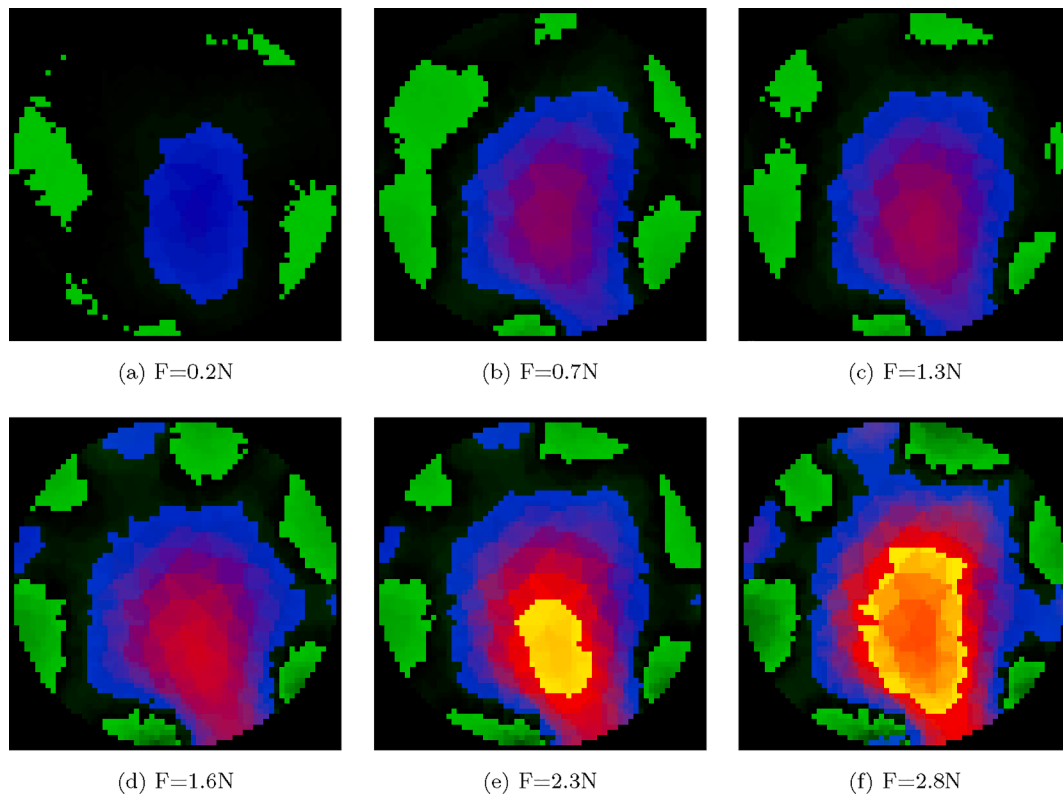


Fig. 4. Functional EMG images generated from the raw signals, Subject 1.

Table 3
Mean correlation coefficients and RMSE for each subject, using logarithmic model with image features.

Subject	Logarithmic Model	
	Mean R^2	Mean RMSE
1	0.95	0.26
2	0.87	0.25
3	0.90	0.29
4	0.89	0.12
5	0.93	0.17
6	0.87	0.20
7	0.95	0.34
All	0.91	0.23

Table 4
Mean correlation coefficients and RMSE for each subject, ViT model.

Subject	Logarithmic Model	
	Mean R^2	Mean RMSE
1	0.97	0.29
2	0.91	0.32
3	0.94	0.31
4	0.93	0.18
5	0.95	0.19
6	0.95	0.20
7	0.97	0.37
All	0.93	0.23

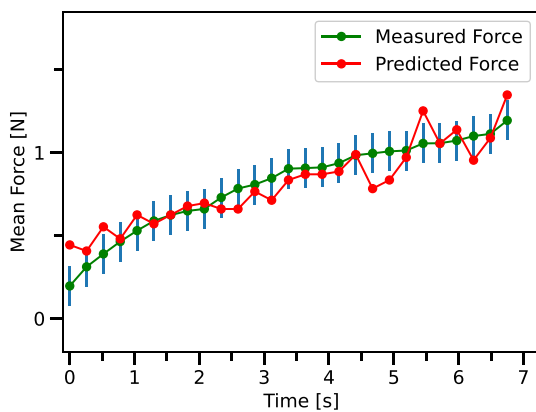


Fig. 5. An example of the force estimated over the course of a single compression using the reconstructed images Subject 4.

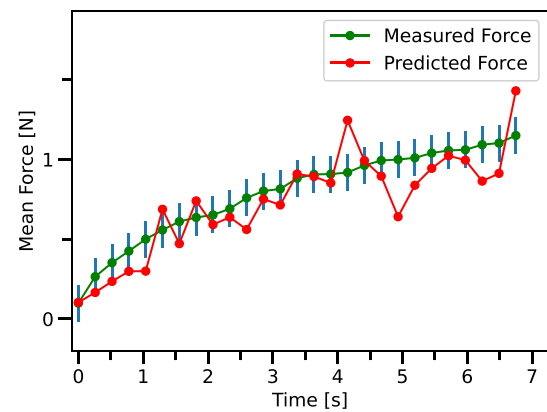


Fig. 6. An example of the force estimated over the course of a single compression using the ViT model Subject 4.

in some sense. Hypothesis testing showed that the mean correlation coefficients of the image-based method are significantly higher than those obtained using in MAV method.

Finally, a ViT network was trained to estimate the force using the reconstructed images. Hypothesis testing showed the correlation coefficients obtained using the reconstructed images were significantly higher than those obtained when using the ViT network to estimate. However, the difference could not be shown to be significant when assuming a difference of 4% or greater. We believe that using a ViT network to estimate the force leads to sufficiently accurate force estimations.

In their work Huang et al. (2017) [25] presented an algorithm isometric force estimation. Their algorithm uses non-negative matrix factorization-based methods to extract activation signals which are used to fit a second-order polynomial. Using this method they achieved a mean correlation coefficient of 0.91 and mean RMSE of 0.23 on a cohort of $N = 12$ participants. We note that these results were obtained using EMG signal measured from a high-density array containing one hundred and twenty-eight electrodes. Comparatively, we used eight electrodes which significantly reduces the cost and complexity of our setup.

Similarly Clancy and Hogan (1997) [37] used a third-order polynomial to estimate torque of the elbow flexor–extensor. The EMG signals were collected using five electrodes placed on the elbow. They reported a standard error of approximately 3% on a cohort of $N = 3$ participants. Our standard error was approximately 0.3% from both the MAV and EMG-image-based models.

It must be noted that the results presented from the two logarithmic models are subject-dependent and, thus, cannot indicate that a specific set of model parameters generalizes to all subjects. Yet, the results of the ViT experiments conversely are reported on hold-out validation set. Nevertheless, the ultimate goal of this research is to obtain a general functional assessment of the EMG signals of the forearm, as opposed to an algorithm or device that must generalize to all users. The preliminary results presented here indicate that the logarithmic model is an appropriate choice for modeling the EMG–force relationship. Due to the small number of participants, one can argue that these results require further research to be statistically significant. Thus, a larger cohort of participants, including rehabilitation patients, is required to validate these discoveries as well as test the generalizability of the model.

Several works discuss image reconstruction using surface electrode measurements. Xi et al. (2021) used EMG signals for predicting preterm birth using EMG signals [13]. Van den Doel (2011) [15] performed source localization using EMG signals. Neither of these works nor other of this kind is concerned with force estimation from the reconstructed images and as such, we cannot compare this aspect of our work to others. To the best of our knowledge, this method is completely novel. Though we note that we rather na?vely made use of the EIT reconstruction algorithm. We believe that a more mathematically appropriate approach may provide further advantages.

5. Conclusions

The logarithmic model can accurately model the EMG-hand grip force relation under isometric contraction with monotonically increasing force. The logarithmic model is robust both to noise and to signal features. Notably, the logarithmic function works well with various choices of EMG descriptors, and transformations. We showed that we can reconstruct visually and quantitatively meaningful images from which the force can be estimated. We note that this significant result is obtained using a relatively na?ve reconstruction algorithm. We believe that a more mathematically appropriate approach, e.g source localization, may provide further advantages and further research should explore this avenue.

The ultimate aim of this research is to lay the groundwork for new clinical methods, which could complement MMT in determining muscle health using functional images. To that end, we note that this research

represents a kind of baseline for how these approaches work for subjects with healthy muscles. Future research should validate these results on a wider scale before exploring how these relationships and approaches may change for subjects suffering from muscle disorders. Since muscle disorders affect approximately seven million people each year in the US alone. We believe that resolving the open questions in this work could complement existing clinical methods and improve the quality of life and care of rehabilitation patients.

Ethical approval

Ethical approval was obtained from the Research Ethics Committee of the *Universidad de la República Hospital (Hospital de Clínicas)*, Montevideo, Uruguay, number 032018.

CRediT authorship contribution statement

Betzalel Fialkoff: Formal analysis, Software, Methodology, Investigation, Data curation, Writing - original draft, Visualization. **Harel Hadad:** Methodology, Validation, Investigation, Writing - original draft. **Darío Santos:** Resources, Conceptualization, Writing - review & editing. **Franco Simini:** Conceptualization, Writing - review & editing. **Marcelo David:** Conceptualization, Investigation, Writing - original draft, Supervision, Project administration, Funding acquisition.

Declaration of Competing Interest

The authors declare that they have no known competing financial interests or personal relationships that could have appeared to influence the work reported in this paper.

Acknowledgments

This research was funded by the Lev Academic Center Internal Grant 5779/2.

References

- [1] J. Mackay, G.A. Mensah, *The atlas of heart disease and stroke*, World Health Organization, 2004.
- [2] C. Beaudart, R. Rizzoli, O. Bruyère, J.-Y. Reginster, E. Biver, Sarcopenia: burden and challenges for public health, *Arch. Public Health* 72 (1) (2014) 1–8.
- [3] S.S. Virani, A. Alonso, E.J. Benjamin, M.S. Bittencourt, C.W. Callaway, A.P. Carson, A.M. Chamberlain, A.R. Chang, S. Cheng, F.N. Delling, et al., Heart disease and stroke statistics–2020 update: a report from the american heart association, *Circulation* 141 (9) (2020) e139–e596, <https://doi.org/10.1161/HYP.0000000000000067>.
- [4] P.A. Iaizzo, W.K. Durfee, *Functional force assessment of skeletal muscles*, in: Springer Handbook of Medical Technology, Springer, 2011, pp. 273–287. doi: 10.1007/978-3-540-74658-4_14.
- [5] D.D. Sloboda, D.R. Clafin, J.J. Dowling, S.V. Brooks, Force measurement during contraction to assess muscle function in zebrafish larvae, *J. Visualized. Exp.: JoVE* (77). doi:10.3791/50539.
- [6] O.H. Kristensen, E. Stenager, U. Dalgas, *Muscle strength and poststroke hemiplegia: a systematic review of muscle strength assessment and muscle strength impairment*, *Arch. Phys. Med. Rehabil.* 98 (2) (2017) 368–380.
- [7] J.-I. Yoo, H. Choi, Y.-C. Ha, Mean hand grip strength and cut-off value for sarcopenia in korean adults using knhans vi, *J. Korean Med. Sci.* 32 (5) (2017) 868, <https://doi.org/10.3346/jkms.2017.32.5.868>.
- [8] S.C. Cuthbert, G.J. Goodheart, On the reliability and validity of manual muscle testing: a literature review, *Chiropractic Osteopathy* 15 (1) (2007) 4, <https://doi.org/10.1186/1746-1340-15-4>.
- [9] R. Correa-de Aratujó, M.O. Harris-Love, I. Miljkovic, M.S. Fragala, B.W. Anthony, T. M. Manini, The need for standardized assessment of muscle quality in skeletal muscle function deficit and other aging-related muscle dysfunctions: a symposium report, *Front. Physiol.* 8 (2017) 87. doi:10.3389/fphys.2017.00087.
- [10] G. Kamen, et al., *Electromyographic kinesiology*, Robertson, DGE et al. Research Methods in Biomechanics. Champaign, IL: Human Kinetics Publ doi:10.5040/9781492595809.
- [11] C. Meeker, S. Park, L. Bishop, J. Stein, M. Ciocarlie, Emg pattern classification to control a hand orthosis for functional grasp assistance after stroke, in: 2017 international conference on rehabilitation robotics (ICORR), IEEE, 2017, pp. 1203–1210. doi:10.1109/ICORR.2017.8009413.

- [12] A. Gailey, P. Artemiadis, M. Santello, Proof of concept of an online emg-based decoding of hand postures and individual digit forces for prosthetic hand control, *Front. Neurol.* 8 (2017) 7. doi:0.3389/fneur.2017.00007.
- [13] Q. Xi, Z. Fu, W. Wu, H. Wang, Y. Wang, A novel localized collocation solver based on trefftz basis for potential-based inverse electromyography, *Appl. Math. Comput.* 390 (2021), 125604, <https://doi.org/10.1016/j.amc.2020.125604>.
- [14] W. Wu, H. Wang, P. Zhao, M. Talcott, S. Lai, R.C. McKinstry, P.K. Woodard, G.A. Macones, A.L. Schwartz, A.G. Cahill, et al., Noninvasive high-resolution electromyometrial imaging of uterine contractions in a translational sheep model, *Science translational medicine* 11 (483). doi:10.1126/scitranslmed.aau1428.
- [15] K. Van Den Doel, U.M. Ascher, D.K. Pai, Source localization in electromyography using the inverse potential problem, *Inverse Prob.* 27 (2) (2011), 025008, <https://doi.org/10.1088/0266-5611/27/2/025008>.
- [16] P.S. Cuculich, Y. Wang, B.D. Lindsay, R. Vijayakumar, Y. Rudy, Noninvasive real-time mapping of an incomplete pulmonary vein isolation using electrocardiographic imaging (ecgi), *Heart Rhythm* 7 (9) (2010) 1316, <https://doi.org/10.1016/j.hrthm.2009.11.009>.
- [17] P.S. Cuculich, J. Zhang, Y. Wang, K.A. Desouza, R. Vijayakumar, P.K. Woodard, Y. Rudy, The electrophysiological cardiac ventricular substrate in patients after myocardial infarction: noninvasive characterization with electrocardiographic imaging, *J. Am. Coll. Cardiol.* 58 (18) (2011) 1893–1902, <https://doi.org/10.1016/j.jacc.2011.07.029>.
- [18] E. Santos, F. Simini, Comparison of electrical impedance tomography reconstruction techniques applied to impetom system, in: 13th IEEE International Conference on Bioinformatics and BioEngineering IEEE, 2013, pp. 1–4.
- [19] E.L. Costa, R.G. Lima, M.B. Amato, Electrical impedance tomography, *Yearbook of Intensive Care and Emergency Medicine* (2009) 394–404, <https://doi.org/10.1097/mcc.0b013e3283220e8c>.
- [20] B.H. Brown, Electrical impedance tomography (EIT): a review, *J. Med. Eng. Technol.* 27 (3) (2003) 97–108.
- [21] M. Bodenstern, M. David, K. Markstaller, Principles of electrical impedance tomography and its clinical application, *Crit. Care Med.* 37 (2) (2009) 713–724.
- [22] W.R. Hendee, S. Chien, C.D. Maynard, D.J. Dean, The national institute of biomedical imaging and bioengineering: history, status, and potential impact, *Ann. Biomed. Eng.* 30 (1) (2002) 2–10.
- [23] A.P. Calderón, On an inverse boundary value problem, *Comput. Appl. Math.* 25 (2006) 133–138.
- [24] D. Staudenmann, I. Kingma, A. Daffertshofer, D.F. Stegeman, J.H. van Dieën, Improving EMG-based muscle force estimation by using a high-density EMG grid and principal component analysis, *IEEE Trans. Biomed. Eng.* 53 (4) (2006) 712–719.
- [25] C. Huang, X. Chen, S. Cao, B. Qiu, X. Zhang, An isometric muscle force estimation framework based on a high-density surface emg array and an nmf algorithm, *J. Neural Eng.* 14 (4) (2017), 046005, <https://doi.org/10.1088/1741-2552/aa63ba>.
- [26] M. Hakonen, H. Piitulainen, A. Visala, Current state of digital signal processing in myoelectric interfaces and related applications, *Biomed. Signal Process. Control* 18 (2015) 334–359, <https://doi.org/10.1016/j.bspc.2015.02.009>.
- [27] R. Barański, A. Kozupa, Hand grip-emg muscle response., *Acta Physica Polonica, A.* 125. doi:10.12693/APhysPolA.125.A-7.
- [28] A. Phinyomark, P. Phukpattaranont, C. Limsakul, Feature reduction and selection for EMG signal classification, *Expert Syst. Appl.* 39 (8) (2012) 7420–7431.
- [29] C.J. De Luca, Surface electromyography: Detection and recording, *DelSys Incorporated* 10 (2) (2002) 1–10.
- [30] A. Adler, W.R. Lionheart, Uses and abuses of EIDORS: an extensible software base for EIT, *Physiol. Meas.* 27 (5) (2006) S25.
- [31] A. Dosovitskiy, L. Beyer, A. Kolesnikov, D. Weissenborn, X. Zhai, T. Unterthiner, M. Dehghani, M. Minderer, G. Heigold, S. Gelly, et al., An image is worth 16x16 words: Transformers for image recognition at scale, arXiv preprint arXiv:2010.11929.
- [32] N. Carion, F. Massa, G. Synnaeve, N. Usunier, A. Kirillov, S. Zagoruyko, End-to-end object detection with transformers, *European Conference on Computer Vision, Springer* (2020) 213–229.
- [33] N. Parmar, A. Vaswani, J. Uszkoreit, L. Kaiser, N. Shazeer, A. Ku, D. Tran, Image transformer, *International Conference on Machine Learning, PMLR* (2018) 4055–4064.
- [34] P. Wang, Implementation of vision transformer, URL: <https://github.com/lucidra/ns/vit-pytorch> (2020).
- [35] A. Vaswani, N. Shazeer, N. Parmar, J. Uszkoreit, L. Jones, A.N. Gomez, L. Kaiser, I. Polosukhin, Attention is all you need, arXiv preprint arXiv:1706.03762.
- [36] G. Research, Vision transformer, URL: https://github.com/google-research/vision_transformer (2020).
- [37] E.A. Clancy, N. Hogan, Relating agonist-antagonist electromyograms to joint torque during isometric, quasi-isotonic, nonfatiguing contractions, *IEEE Trans. Biomed. Eng.* 44 (10) (1997) 1024–1028.